Article

Not peer-reviewed version

Tailoring Alginate-Gelatin Hydrogels to Precisely Modulate Osteogenesis in Dental Pulp Stem Cells While Preserving Other Cellular Behaviors

Zied Ferjaoui *, Roberto López-Muñoz, Soheil Akbari, Fatiha Chandad, Mantovani Diego, Mahmoud Rouabhia, Roberto Fanganiello

Posted Date: 27 March 2024

doi: 10.20944/preprints202403.1674.v1

Keywords: alginate; gelatine; hydrogel; stiffness; DPSCs and Osteogenic differentiation

Article

Tailoring Alginate-Gelatin Hydrogels to Precisely Modulate Osteogenesis in Dental Pulp Stem Cells While Preserving Other Cellular Behaviors

Zied Ferjaoui [1,*], Roberto López-Muñoz [2], Soheil Akbari [3], Fatiha Chandad [1], Diego Mantovani [2], Mahmoud Rouabhia [1] and Roberto Fanganiello [1]

[1] Oral Ecology Research Group, Faculté de Médecine Dentaire, Université Laval, Québec City, Canada
[2] Laboratory for Biomaterials and Bioengineering, CRC-I, Dept Min-Met-Mater Eng, & CHU de Québec, Regenerative Medicine, Laval University, Québec City, Canada
[3] Département de génie chimique, Université Laval, Québec, QC G1V 0A6, Canada
* Correspondence: ferjaoui1zied@gmail.com

Abstract: Alginate-gelatin (Alg-Gel) hydrogels have been used experimentally but not clinically associated with mesenchymal stromal / stem cells (MSCs) to guide bone tissue formation. One of the main challenges for its clinical application is optimizing Alg-Gel stiffness to guide osteogenesis. In this study, we investigated how Alg-Gel stiffness could modulate the dental pulp stem cell (DPSCs) attachment, morphology, proliferation, and osteogenic differentiation, identifying the optimal condition to uncouple osteogenesis from the other cell behaviors. An array of Alg-Gel hydrogels was prepared by casting different percentages of Alg and Gel being crosslinked with 2 % CaCl2. We selected two hydrogels, one with 11± 1 kPa called "low" stiffness and one with 55 ± 3 kPa called "high" stiffness. Hydrogel analyses showed that the average swelling rates were 20 ± 3% for low and 35 ± 2% for high hydrogels. The degradation percentage was 47 ± 5% and 18 ± 2% for low and high hydrogels, respectively. Both hydrogel types showed homogeneous surface shape and protein (Alg-Gel) interaction with $CaCl_2$ as assessed by FTIR-ATR and XPS. Cell culture showed good adhesion of the DPSCs to the hydrogels and proliferation. Furthermore, better osteogenic activity was obtained with high-stiffness hydrogels. In summary, this study confirms the possibility of characterizing and optimizing the stiffness of alginate-gelatin gel to guide osteogenesis in vitro without altering other cellular properties of DPSCs.

Keywords: alginate; gelatine; hydrogel; stiffness; DPSCs and Osteogenic differentiation

1. Introduction

Mesenchymal stromal/stem cells (MSCs) hold great potential in regenerative medicine because they differentiate into various cell types, including osteoblasts, responsible for bone tissue formation and regeneration[1]. Bone regeneration requires osteogenic cells and a scaffold to support the cells forming bone tissue. Alginate and gelatin hydrogels have emerged as promising biomaterials for tissue engineering applications due to their biocompatibility and ability to promote cell adhesion and differentiation[2],[3]. However, while several studies have shown the osteogenic potential of these hydrogels, very few have examined the effect of hydrogel stiffness on MSCs osteogenic differentiation. Furthermore, it is essential to design hydrogels that selectively promote osteogenesis without adversely impacting other cell behaviors, such as MSCs cell differentiation to non-osteogenic lineages. It also has been shown that the proliferation and osteogenic function of the osteoblasts fluctuated with increasing gelatin concentration in gelatin-nano-hydroxyapatite microcapsules (nHA), suggesting that the hydrogel properties must be balanced to provide an effective 3D osteoconductive microcapsule[4]. The alginate (1%)-gelatin (2.5%)-nHA (0.5%) microcapsule with a compressive modulus of 0.19 MPa ± 0.02 revealed maximum performance for cell proliferation and function, indicating a potential microcapsule composition to prepare building blocks for modular bone tissue engineering[4]. In another study, the effects of substrate stiffness on the differentiation of hMSCs, derived from the adult human bone marrow into adipogenic and osteogenic cells has shown

 doi:10.20944/preprints202403.1674.v1

that adipogenic and osteogenic differentiation of hMSCs is likely to occur on a substrate with stiffness similar to that of their in vivo microenvironments[5]. In the same sense, Žigon-Branc et al. [6] evaluated how the stiffness of gelatin-based hydrogels (having a storage modulus of 538, 3584, or 7263 Pa) affects the proliferation and differentiation of microspheroids formed from telomerase-immortalized human adipose-derived stem cells (hASC/hTERT). They showed better cell differentiation with calcium deposits when using softer hydrogels, suggesting that these soft hydrogels promote osteogenesis. The authors concluded that the encapsulation of adipose-derived stem cell microspheroids in gelatin-based hydrogels has promising potential for future applications for bone regeneration. A cell imprinted poly(dimethylsiloxane)/hydroxyapatite nanocomposite substrate was fabricated to engage topographical, mechanical, and chemical signals to stimulate and promote osteogenic differentiation of stem cells was developed by Kamguyan et al.[7]. showing that the simultaneous roles of surface patterns and substrate viscoelastic properties modulate stem cell differentiation toward osteogenic phenotypes. To better understand the regulation of cell differentiation by mechanical signals, Witkowska-Zimny et al [8], investigated the influence of matrix stiffness (E = 1.46 kPa and E = 26.12 kPa) on the differentiated osteogenic cell line of bone marrow stem cells (BM-MSCs) and bone-derived cells (BDCs) using flexible polyacrylamide substrates coated with collagen. They found that substrate stiffness can regulate osteogenic differentiation, which may depend on commitment to multi- or unipotent target cells. Osteogenic differentiation of BM-MSCs was greater on a rigid substrate than on a soft substrate, whereas osteogenic differentiation of BDCs did not vary with substrate stiffness. These data highlight the role of external mechanical determinants in stem cell differentiation and may be useful in translating the approach to functional tissue engineering. These previous studies have investigated cell proliferation and differentiation by culturing stem cells on hydrogel substrates with controllable stiffness. However, it would be particularly important to understand the influence of mechanical properties on stem cell behavior in terms of osteogenic growth factor, as cell behavior may differ depending on substrate stiffness.

The ideal biomaterial to form a reliable hydrogel must be biocompatible, biodegradable, and non-toxic to promote cell adhesion, growth, and differentiation [9],[10]. Alginate is a natural polysaccharide approved by the FDA and widely used as a "smart" biomaterial and as a bio-ink when loaded with cells [11],[12]. Alginate is often combined with bioactive molecules or other polymers to enable cell adhesion and proliferation[13]. The combination of sodium alginate and gelatin makes them useful for cell culture[14],[15]. Alginate provides a porous structure that allows the diffusion of nutrients and growth factors, while gelatin offers a favorable surface for cell adhesion and differentiation[16]. Studies have demonstrated that hydrogels composed of alginate and gelatin can promote osteogenic differentiation of mesenchymal stem cells, contributing to bone formation [14],[15]. Therefore, alginate-gelatin hydrogels are considered good candidates for osteogenic differentiation due to their biocompatibility and surface properties that promote cell adhesion and differentiation, as well as their ability to induce the differentiation of mesenchymal stem cells into osteoblasts[17],[18]. Despite advances in research on alginate and gelatin hydrogels, few studies have investigated the influence of their stiffness on the expression of osteogenic markers of DPSC cells, such as osteocalcin, alkaline phosphatase, and type I collagen[15],[19]. The expression of these markers is used as an indicator of the osteogenic differentiation of DPSC cells[19]. Therefore, studying the expression of these markers as a function of the stiffness of the alginate-gelatin hydrogel is important in developing a hydrogel that can guide the osteogenic differentiation of DPSCs based on its stiffness[20].

The objective of this study was to differentiate DPSCs and MG-63 (cells derived from osteosarcoma (used as a positive control)) into osteoblast-like cells and to study their interaction with hydrogels of different stiffness (Figure 1). Our approach is based on enhancing the mechanical properties of hydrogels by adjusting the ratios of alginate and gelatin. We have fine-tuned the stiffness of hydrogels to specific targets, notably around 11±1 kPa and 55±3 kPa, enhancing their applicability without affecting cell adhesion, proliferation, or morphology. Interestingly, we observed a significant enhancement in osteogenic differentiation on the stiffer hydrogels, as demonstrated by increased Alizarin Red staining and alkaline phosphatase activity, suggesting

 doi:10.20944/preprints202403.1674.v1

potential in guiding tissue engineering outcomes. Therefore, this newly developed hydrogel with optimized stiffness can promote the adhesion and growth of osteogenic cells, forming bone tissue for clinical applications.

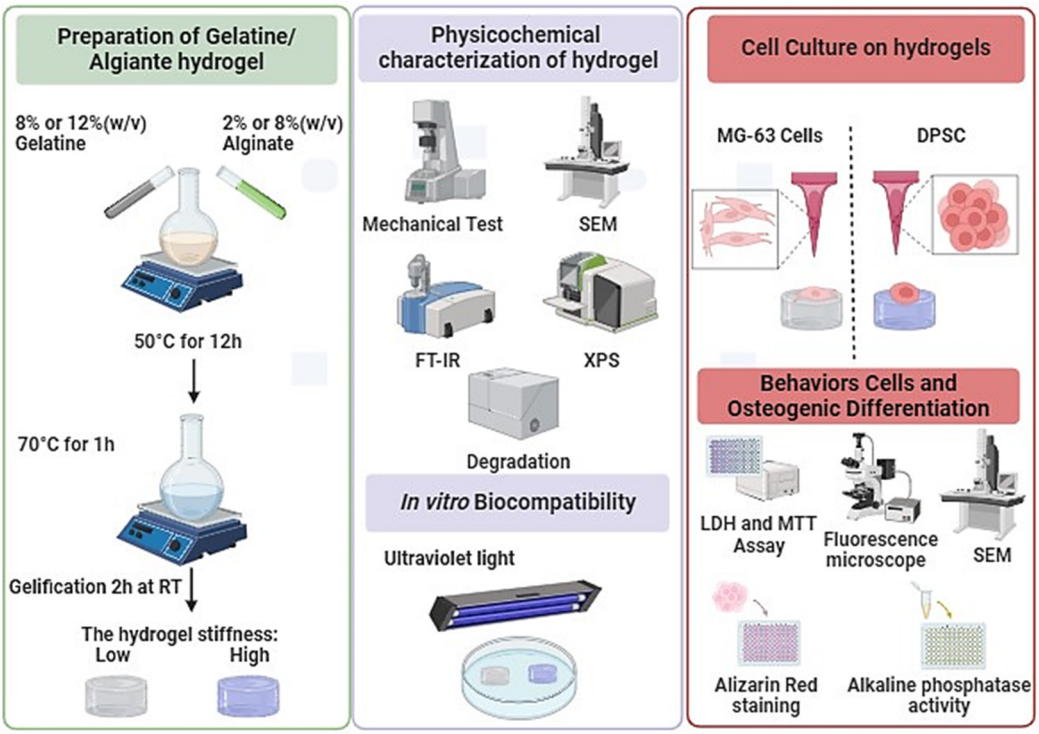

Figure 1. Synthesis, Characterization, and Cell Culture on Low and High Stiffness Hydrogels. This figure can be used as a graphical abstract figure.

2. Materials and Methods

2.1. Materials

Sodium alginate (W201502), gelatin (type A: from porcine skin), calcium chloride dihydrate (ReagentPlus®, ≥ 99.0 %), calcium chloride, phosphate-buffered saline (PBS) and Ascorbic Acid-2-Phosphate were obtained from Sigma-Aldrich (St. Louis, MO, USA). For cell culture experiments, Dulbecco's Modified Eagle Medium F12 (DMEM F12), L-Glutamine (200 mM), Antibiotic/Antimycotic Solution (Pen/Strep/Fungiezone), Fetal Bovine Serum (FBS) and Dexamethasone (98%) was purchased from Thermo Fischer Scientific (Waltham, MA, USA).

2.2. Preparation of Alginate-Gelatin Hydrogels

Two types of hydrogels based on different percentages of Alg/Gel were prepared: one composed of 2 % (w/v) of alginate and 8 % (w/v) of gelatin, and the second one composed of 8 % (w/v) of alginate and 12 % (w/v) of gelatin. Both were prepared in PBS (0.1 M, pH 7.4). The different solutions were placed in a water bath at 50 °C overnight to dissolve the polymers and homogenize the solutions. Then, a pasteurization process was performed at 70 °C for 1 h for all experiments. To obtain hydrogel samples, 3 mL of Alg/Gel solution was added to a 6-well plate and left at room temperature for 2 h to promote complete gelation. The samples were then sliced with a sterile scalpel blade into 1 x 1 cm squares. All the samples were immersed in a 2 % $CaCl_2$ solution for 1 h for crosslinking. Finally, the samples were washed with deionized water to remove excess CaCl2 and were stored at 4 °C for further use.

 doi:10.20944/preprints202403.1674.v1

2.3. Hydrogels Physicochemical Characterizations

Surface morphology observations of the hydrogels were performed by scanning electron microscopy (SEM) on a Quanta 250, FEI Company Inc. (Thermo-Fisher Scientific, OR, USA), operated at 5kV/6 spot in secondary electron mode. Before scanning, all samples were immersed in liquid nitrogen for 60 s, freeze-dried for 24 h and sputter-coated with gold for 2 min to avoid surface burning.

Complementary analysis of the functional groups on hydrogels was determined by Fourier-transform infrared-attenuated total reflectance (FTIR-ATR) spectroscopy, using an Agilent Cary 660 FTIR (Agilent Technologies, Santa Clara, CA, USA). All measurements were obtained in absorbance mode and 128 scans were recorded between 500 and 4000 cm-1 with a spectral resolution of 4 cm-1. All samples were partially dried at room temperature and measured to confirm the chemical composition. The chemical composition of the scaffolds and the crosslinking with $CaCl_2$ was assessed by X-ray photoelectron spectroscopy (XPS) using a PHI 5600-ci equipment (Physical Electronics, MN, USA). Before the measurements, the samples were freeze-dried for 24 h, and each sample was scanned at three different positions to observe the homogeneity of the crosslinking.

2.4. Rheological Characterizations

All rheological measurements were performed using a rheometer (DHR-3, TA Instruments) with parallel plate geometry and a diameter of 20 mm. Circular hydrogels were obtained from crosslinked samples by puncturing the hydrogels with a steel hollow punch with an internal diameter of 20 mm. Sandpaper (80 grit) was pasted on the surface of the parallel plates to avoid the samples' slipperiness during the measurements[21]. Storage modulus (G') and loss modulus (G'') were measured on an amplitude sweep oscillatory test ranging from 0.1 to 10 % strain using an angular frequency of 1 rad/s at 37 °C. A thermal sweep test in the linear viscoelastic range at 0.5 % strain with an angular frequency of 1 rad/s was performed from 10 °C to 40 °C. Moreover, the crosslinking behavior was tested through frequency sweep experiments from 0 to 100 rad/s applying 0.5 % strain at 37 °C.

2.5. Swelling

The lyophilized hydrogel samples were weighed (W0). To determine the swelling of the hydrogel, the samples were immersed in 3 mL of PBS (pH 7.4) for 24 hours at 37 °C to reach equilibrium. The swollen hydrogel was weighed as (W1) after absorbing the excess solution on the hydrogel with filter paper. Finally, the swelling rate of the hydrogels was calculated using the following formula: swelling rate (%) = (W1-W0)/W0 × 100%.

2.6. Degradation Behavior

The hydrogels degradation was investigated by immersing the samples in 3 mL of PBS and incubating them at 37 °C. The initial mass (W0) was measured, and the hydrogels were weighed at different times (W1: 7, W2 :14, and W3 :21 days). The remaining mass (wet weight, %) was calculated using the following equation: remaining (%) = W1/W0 × 100 %.

2.7. Cell Culture

For sterilization, the hydrogels were soaked in 70% ethanol in the presence of ultraviolet (UV) light for 30 min and then washed with sterile PBS. Sterile Alg-Gel hydrogels were placed in wells of six-well plates and incubated in DMEM/F12 supplemented with 1% (v/v) penicillin/streptomycin at 37 °C overnight (hydrogel preconditioning) before cell seeding. Cells (DPSC and MG-63) were seeded onto the surface of each hydrogel by applying 50 µL of medium containing 2.105 cells on the surface of each hydrogel, incubated for 2 h in a humidified incubator at 37°C and 5% CO_2. At the end of this incubation period, 1 mL of culture medium was added to each hydrogel, and cells were cultured for (7, 14, and 21 days). To promote osteoblastic differentiation, the culture medium was supplemented with 100 µM l-ascorbic acid 2-phosphate and 10-7 M of dexamethasone osteoinductive medium

 doi:10.20944/preprints202403.1674.v1

(OM). DPSCs from 4 - 6 passages and MG-63 from 10 - 12 passages were used to characterize cell attachment, proliferation, and differentiation.

2.7.1. osteoblast Adhesion

Hydrogel samples were inserted into wells of 12-well plates, and then the cells were seeded (5.10^4) and cultured for 1, 3, and 7 days. At the end of each culture period, the hydrogels were washed twice with PBS, and then the cells were fixed using 4% formaldehyde (Sigma Aldrich, USA) at room temperature for 60 min. The fixed cells were washed with PBS and stained with Hoechst 33342 (Thermo Scientific, USA) for 15 minutes. Hydrogels were washed 3 times X 2 min with distilled water, and images were captured using an Olympus FSX100 fluorescence microscope and visualized with the FSX-BSW imaging software (Olympus, Tokyo, Japan).

2.7.2. Cell Viability

Following culture for 1, 3, 7, 14, and 21 days on the Alg-Gel hydrogels, the viable cells were determined. Briefly, 5.10^4 cells were grown on the hydrogels in a 12-well plate for the required periods, followed by washing with PBS. The cells were detached from the hydrogels using 0.25 % (w/v) trypsin-EDTA. The cells were washed twice with a culture medium, then suspended in 1 mL of a culture medium, and mixed thoroughly. We mixed 10 µL of each cell suspension to count viable cells with 10 µL of trypan blue solution. This mixture was transferred into a hemocytometer chamber and counted under an optical microscope to determine viable cells (bleu trypan unstained cells) and dead cells (trypan bleu-stained cells). Cell viability was further assessed by MTT [3-(4,5-dimethylthiazol-2- yl)-2,5-diphenyl-2H-tetrazolium bromide] assays performed according to the manufacturer's protocol (Roche Diagnostics, Manheim, Germany), which measures the capacity of mitochondrial dehydrogenase in viable cells to reduce MTT to purple formazan crystals. After each culture period (1, 3, 7, 14, and 21 days), the medium was supplemented with 10% MTT chemical and incubated at 37 °C for 3 h. Subsequently, excess MTT was removed by two washes, and the formazan present in live cells was solubilized isopropanol-0.04% HCl solution. Finally, 200 µL in triplicate of the supernatant was transferred from each hydrogel to wells of a 96-well flat-bottom plate, and the absorbance at 550 nm of the formazan dye was determined with a microplate spectrophotometer reader (X-Mark microplate spectrophotometer (Bio-Rad).

2.7.3. Cytotoxicity Assessment

Cytotoxicity was examined using a lactate dehydrogenase (LDH) assay. DPSCs and MG-63 cells were cultured on hydrogels in 12-well plates (5×10^4 cells/well) for 1, 3, 7, 14, and 21 days[22]. After each culture period, the medium was collected and stored at -80°C to assess cellular damage, which was measured by LDH release. Briefly, 10 µL of the culture supernatant was transferred to a 96-well plate, and the enzymatic reaction was performed following the instructions of the LDH cytotoxicity assay kit (Roche Diagnostics, Manheim, Germany). Next, 100 µL of the LDH reaction mixture was added to each well, and the plate was incubated in the dark for 30 minutes at room temperature. After that, 10 µL of stop solution was added to stop the reaction. The absorbance was measured at 450 nm using an X-Mark microplate spectrophotometer (Bio-Rad). The experiment included negative, positive, and background controls for total LDH activity.

2.7.4. Cells Morphology

SEM was used to study the morphology of DPSCs and MG-63 cells after 14 days of culture on the hydrogels. Following cell culture, the hydrogels were fixed in a solution of 0.2% alcian blue, 0.2% red ruthenium, and 2.5% glutaraldehyde in 0.1 M cacodylate buffer (pH 7.2) for 4 hours at room temperature. This step was repeated one more time. After fixation, the samples were sputtered with gold and observed under a JEOL 6360 LV scanning electron microscope (Soquelec Inc., Montreal, QC, Canada) at an accelerating voltage of 15 kV.

 doi:10.20944/preprints202403.1674.v1

2.8. Osteogenic Activity

DPSCs and MG63 cells (at a density of 2×10^5 cells) were cultured on the different hydrogels for 7, 14, and 21 days. At the end of each culture period, the supernatant was collected and used to measure the activity of alkaline phosphatase (ALP) (Alkaline Phosphatase Assay Kit, No. ab83369, Abcam, Canada) according to the manufacturer's protocol. Briefly, 80 µL of each supernatant was transferred, in technical triplicates, to wells of a 96-well flat-bottom plate and was incubated with 50 µL of 5 mM pNPP solution for 60 min at room temperature, followed by adding 20 µL of Stop Solution to stop the conversion of p-nitrophenol into p-nitrophenylate. The absorbance was determined by a BioRad microplate reader at 405 nm. The Alg-Gel hydrogels were fixed with 4 % formaldehyde for 60 min at room temperature and then stained with Alizarin Red S Staining (ARS) (Sigma-Aldrich - USA) to evaluate the mineralization after 7, 14, and 21 days. Briefly, 500 µL of cetylpyridinium chloride was added to each well and incubated for 15 min at room temperature to dissolve the calcium nodules. The OD value was measured at a wavelength of 550 nm using a BioRad microplate reader. The results were normalized to a determined number of viable cells (10^6 cells).

2.9. Statistical Analysis

The values were reported as the means ±SDs for each analysis based on six experiments. To test the significance of the observed difference between the experimented groups, an unpaired student t-test (except otherwise stated) was applied, with a value of $p < 0.05$ considered to be statistically significant.

3. Results and Discussion

3.1. Preparation and Characterization of Alg-Gel Hydrogels

To examine the gelation of the hydrogels, photographs of the vials in the reverse reaction mode were taken before and after the completion of the process, as shown in Figure 2a. No movement was observed in the solution after 2 h of incubation at 22°C, indicating complete gelation. The structural analysis using SEM showed that both hydrogels exhibited a flat and homogeneous surface with no visible pores (Figure 2b).

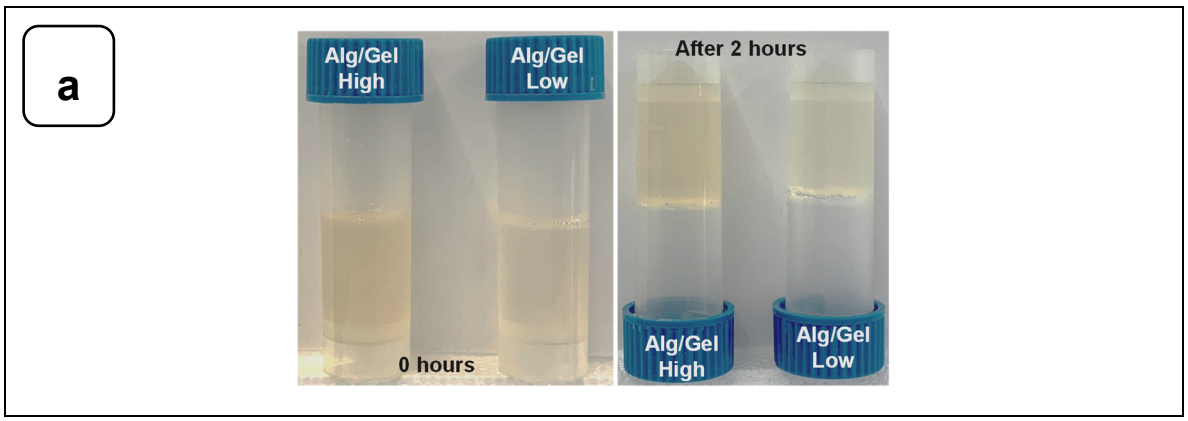

 doi:10.20944/preprints202403.1674.v1

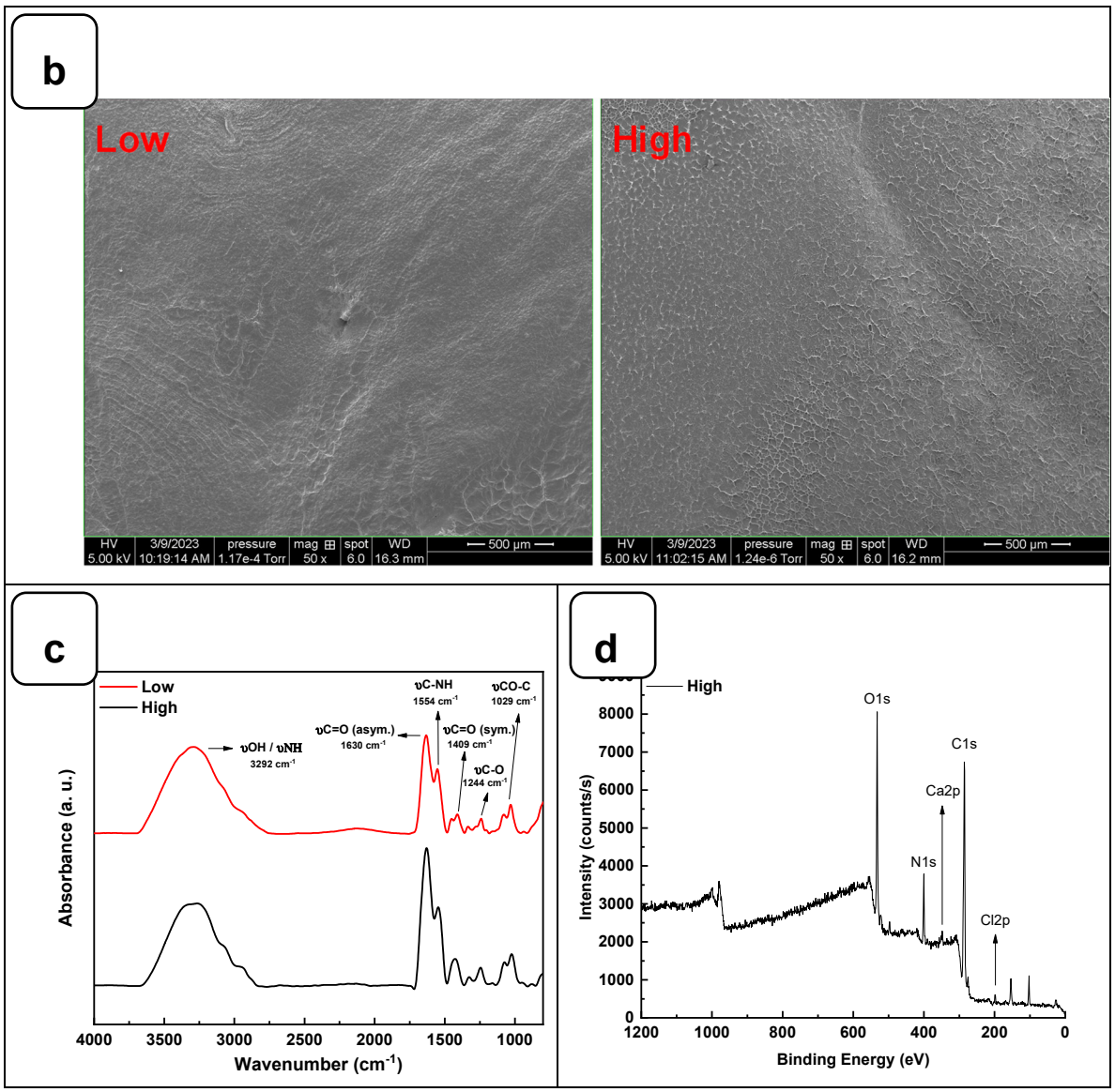

Figure 2. (a) Gelification of Alg-Gel hydrogels after 2 h at room temperature. (b) SEM images of Low and High Alg-Gel hydrogels. (c) FTIR-ATR spectra of Low and High Alg-Gel hydrogels (d) XPS analysis of High hydrogel with $CaCl_2$.

The interaction between the alginate and gelatine contributing to the hydrogel formation was monitored by FTIR-ATR spectroscopy (Figure 2c), confirming the presence of specific absorption bands assigned to the vibrations of the corresponding alginate and gelatine functional groups, as reported previously [23]. The absorption peaks at 1606 cm^{-1} and 1406 cm^{-1} in the infrared spectrum of pure alginate were attributed to the asymmetric stretching vibrations of the alginate groups. In addition, the absorption band at about 1400 cm-1 represents the carboxyl group of gelatins. The two absorption peaks at 1635 cm^{-1} and 1534 cm^{-1} correspond to gelatin's amide I and amide II bands. These changes indicate a strong molecular interaction between the alginate and gelatin chains through the self-organization of polyelectrolyte complexes, including hydrogen bonding and electrostatic attraction[24],[16]. The surface XPS survey spectrum of the hydrogels is shown in Figure 2d and Figure SI 1. C and N are components of Alg and Gel, while Ca refers to calcium chloride is used as a crosslinking agent[23].

The rheological studies for Alg-Gel hydrogels were performed to assess the viscoelastic behavior of the crosslinked hydrogels and obtain two types of hydrogels with low and high stiffness properties. In this case, low-stiffness hydrogels refer to Alg-Gel ratios of 2 %/8 %, while the ratios for high-stiffness hydrogels correspond to 8 %/12 %. Strain sweep tests ranging from 0.1 to 10 % show

 doi:10.20944/preprints202403.1674.v1

the linear viscoelastic region of both formulations at low shear stress and 37 °C (Figure 3a). The storage modulus (G') obtained from the viscoelastic region (Figure 3b) shows a significant difference for high-stiffness hydrogels at around 55.6 ± 0.6 kPa compared to 11.8 ± 0.1 kPa for low-stiffness hydrogels. Similar stiffness values were reported by Chen et al.[25], using 20 % (w/v) of methacrylated gelatin (GelMA) and 3 % (w/v) of sodium alginate. In such a study, the authors promoted a stiffness increase in the dynamic hydrogel from 10 to 68 kPa using UV, $CaCO_3$, and $CaCl_2$ as crosslinkers. Our study showed good reproducibility of the formulations tested to obtain two types of hydrogels with high and low stiffness using as low as 2 % (w/v) of $CaCl_2$ for 1 h to crosslink the alginate.

On the other hand, the thermal sweep experiments of the scaffolds confirmed that the time and crosslinking concentration were enough for both formulations to obtain a hydrogel that does not have a significant change in stiffness, as is shown in Figure 3 c. The volume of the $CaCl_2$ solution and the time used to crosslink all the hydrogels were sufficient to promote an optimal Ca^{+2} ions penetration into the hydrogel structure, as it was evidenced by Naghieh et al.[26]. Additionally, a frequency sweep test was performed to evaluate the impact of the crosslinking conditions on the storage and loss modulus. Figure 3d shows no crossover point at higher frequency ranges. It suggests that G' and G'' values are independent of the frequency, a typical behavior of chemically crosslinked hydrogels[27]. Taking into consideration the temperature sensitivity and the concentration of the gelatin matrix in the scaffolds, the lack of a crossover point could be due to the good distribution and entanglement of the crosslinked polymeric chains of Alg with the Gel chains, avoiding their free movement to flow even at 37 °C. This behavior could be compared with the results obtained by Gregory et al.[28]. In their study, the frequency sweep tests presented an increase of G' and G'' proportional to the frequency with no crossover point when the Alg is at a high molecular weight.

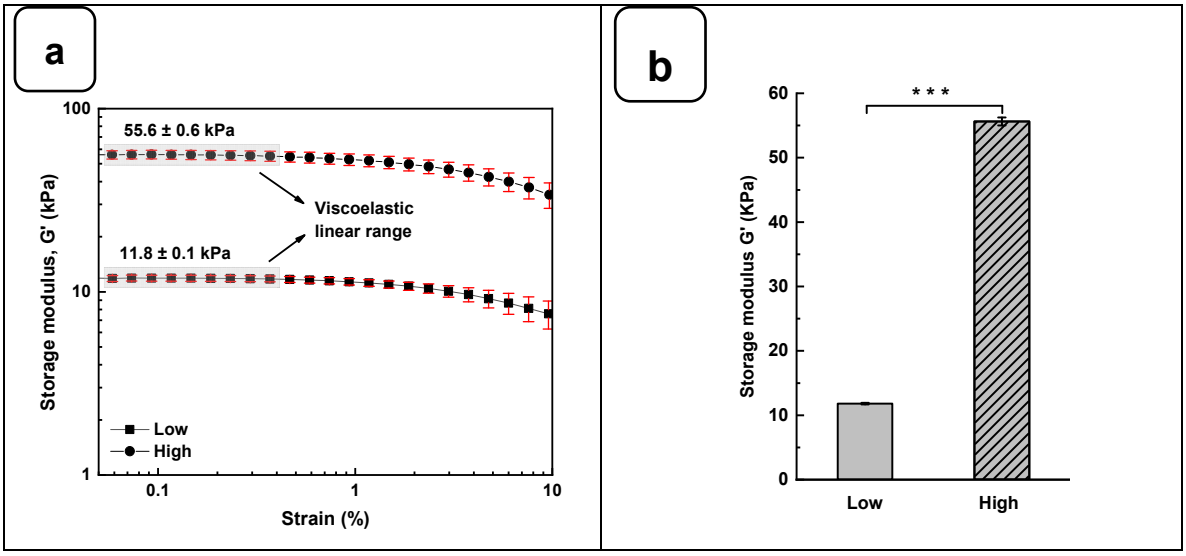

 doi:10.20944/preprints202403.1674.v1

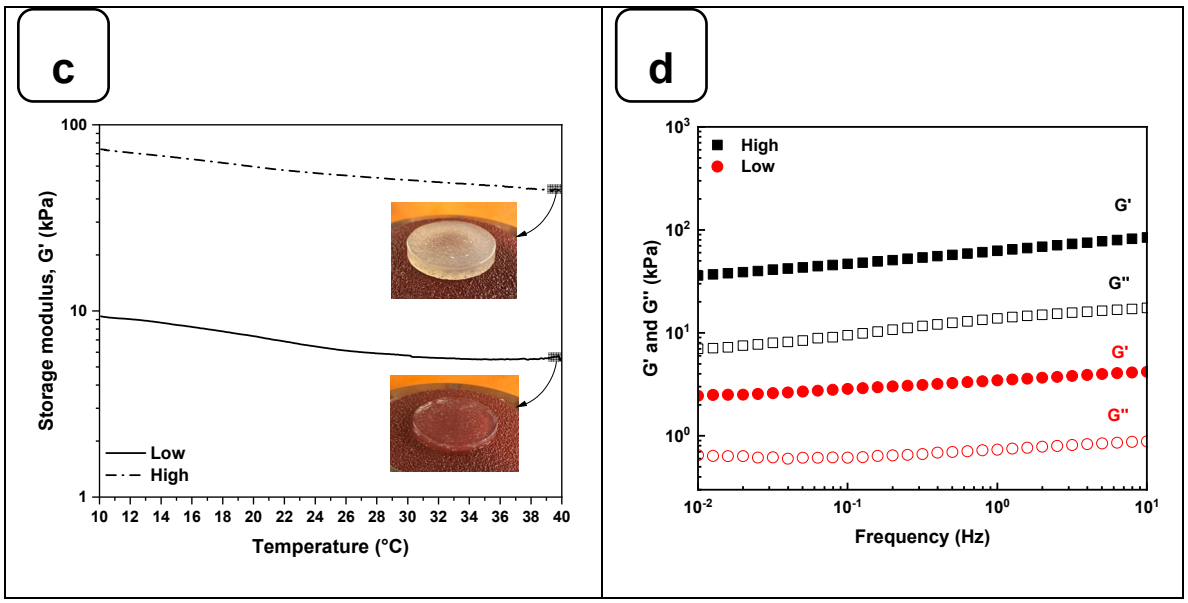

Figure 3. Rheological characterization of Alg-Gel hydrogels for low and high stiffness formulations. (a) Evaluation of the G' and G'' by strain amplitude sweep at 37 °C. (b) Average elastic modulus measured from the linear viscoelastic range. (c) Evaluation of the hydrogel's stability by thermal sweep tests. (d) Frequency sweep tests of low and high-stiffness hydrogels at 37 °C. ***p< 0.001.

Another important factor affecting the mechanical properties of the gels is the tendency to swell. Figure SI 2a shows that the average swelling rates of the low and high hydrogels were 20 ± 3% for "high" and 35 ± 2% for "low". The stability of the hydrogels in PBS at 37ºC was shown in Figure SI 2b. After 7 days of incubation in PBS at 37°C, there was no significant stiffness difference between the two hydrogels. However, after 14 days, a difference was observed, with a higher degradation rate for the low-stiffness hydrogel. This observation was confirmed after 21 days of incubation, with respective degradation percentages of 53 ± 5% and 82 ± 2% for the two hydrogels. These results demonstrate that the degradation and swelling rates depend on the amount of alginate and gelatin and the absence of pores, which can increase the degradation and swelling rates[29].

3.2. Biological Performances ofAlg-Gel Hydrogels

Adhesion is one of the major factors revealing cell behavior. If adherent cells cannot attach due to inappropriate conditions, they will not grow, and finally, they will die. Thus, evaluating osteoblast adhesion to the Alg-Gel hydrogels is important to demonstrate whether the hydrogels are suitable for cell culture. As shown in Figure 4a and Figure SI 4, both DPSC and MG63 cells had good adhesion to all tested hydrogels. The Hoechst staining showed stained cells all over the surface of each hydrogel. The stained cell density was increased from day one to day 21 of the culture, suggesting cell adhesion and proliferation. To confirm such observation, we performed MTT assay to measure cell growth viability at different culture periods. As reported in Figures 4b and 4c the hydrogels promoted osteoblast proliferation. Indeed, with DPSC, absorbances after 7 days of culture were 1.33 ± 0.04 with the "low" hydrogels and 1.29 ± 0.06 with the "high" hydrogels. Similar results were obtained with MG-63 cells cultured for 7 days on the hydrogels, with absorbances ranging from 0.95 ± 0.02 with the "low" hydrogels and 0.82 ± 0.01 with the high hydrogels. At 21 days post-culture, DPSC showed increased absorbances with 1.32 ± 0.09 for "low" hydrogels and 1.11 ± 0.07 for "high" hydrogels. MG-63 also showed better growth at 21 days with an absorbance of 1.12 ± 0.08 with low-stiffness hydrogels and 1.05 ± 0.07 with high-stiffness hydrogels. Overall, this study demonstrated that hydrogel stiffness did not affect osteoblast cell adhesion and proliferation (MG-63 and DPSCs). The proliferation of osteoblasts on alg-gel hydrogels was confirmed by trypan blue exclusion assay. Figures 4d and 4f show that after one day of culture on the hydrogels, the cell count of DPSCs on Low and high hydrogels is 1.5 ± 0.3 10^4 and 1.1 ± 0.2 10^4, respectively. With MG-63, the live cell

 doi:10.20944/preprints202403.1674.v1

numbers were 5.2 ± 0.1 10^4 on Low and 4.7 ± 0.4 10^4 on high hydrogels. After 7 days of culture, the live cell numbers significantly increased, reaching 3.4±0.2 10^5 and 3.0 ± 0.1 10^5 DPSC, while with the MG-63 we had 6.5 ± 0.2 10^5 and 6.1 ± 0.2 10^5 for the low and high hydrogels, respectively. At 21 days of culture, there was no increase in the cell number compared to 7- and 14 days, suggesting cell growth saturating due to the absence of free space for them to proliferate. Our results with Hechest sating, MTT assay, and Trypan blue exclusion assay confirmed that these hydrogels promote cell adhesion, viability, and proliferation with no toxic effect. Indeed, the toxicity was evaluated by an LDH release assay and showed (Figure SI3) no significant increase of the LDH activity when comparing the cell culture or not on each hydrogel type.

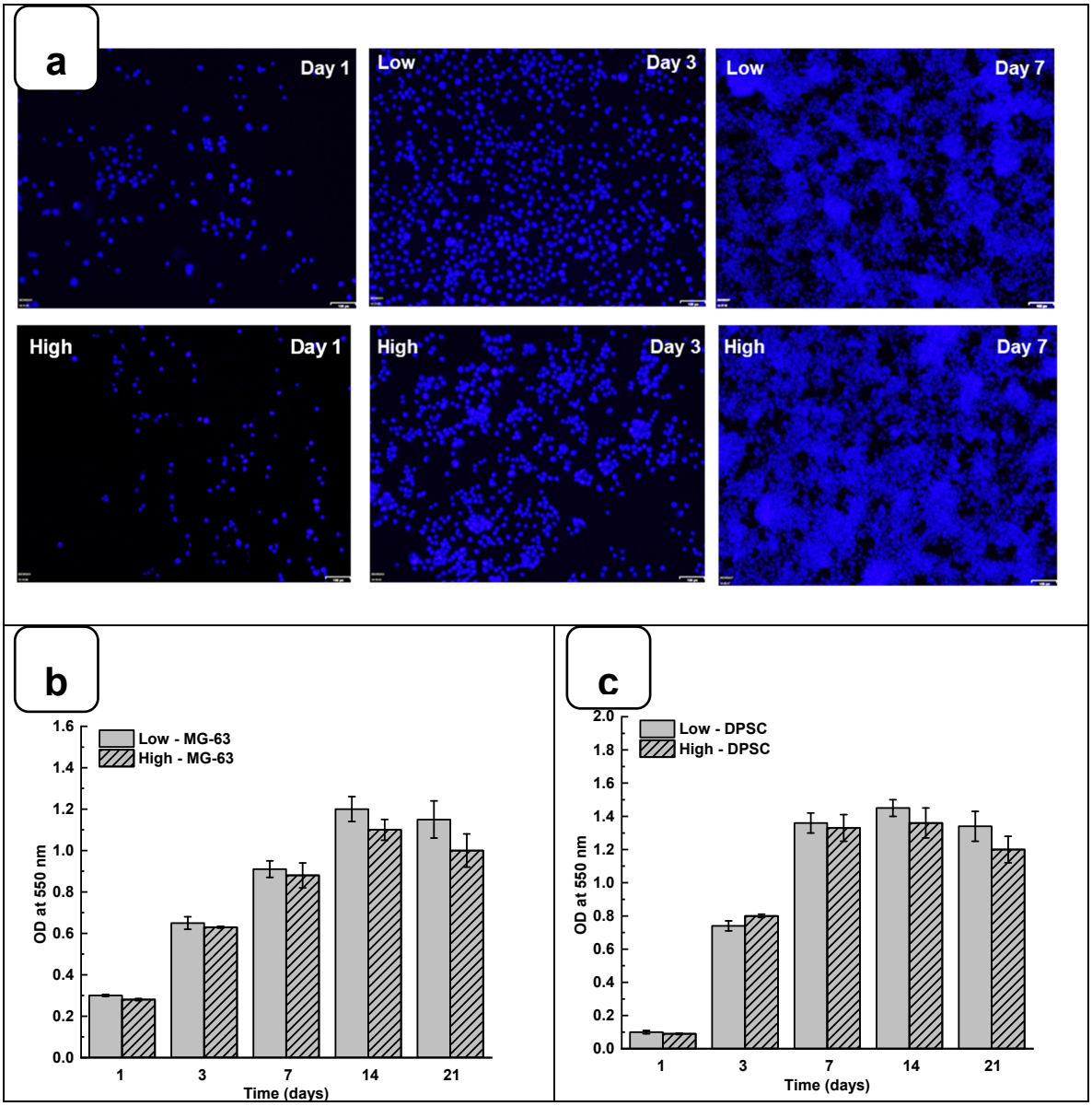

 doi:10.20944/preprints202403.1674.v1

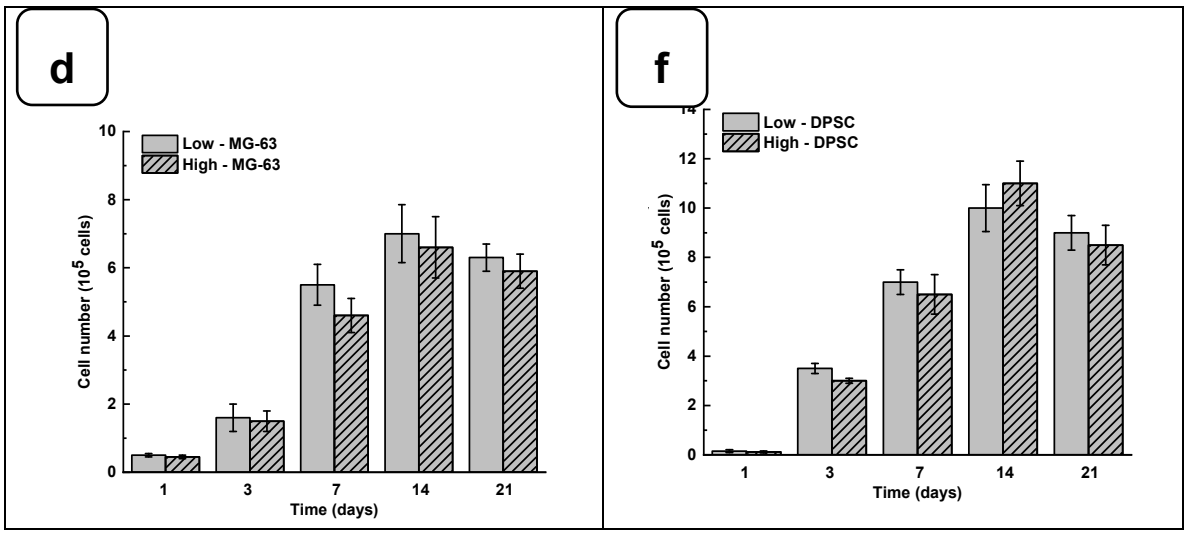

Figure 4. (a) DPSC cells cultured for 1, 3, and 7 days on Low and High hydrogels and stained with Hoechst dye. MTT assay for cells cultured for 1, 3, 7, 14, and 21 days on Low and High hydrogel: (b) MG-63 cells and (c) DPSC. Cell counts of (d) MG-63 and (f) DPSC were cultured on hydrogel for 1, 3, 7, 14, and 21 days. Data points are means of 3 independent experiments in duplicate (±SD).

As the hydrogels were not toxic to the osteoblasts, we also compared the cell adhesion and proliferation obtained with low and high hydrogel stiffness, showing no significant differences. The absence of a significant difference in cell adhesion and proliferation on hydrogels despite a significant difference in stiffness between the low and high hydrogels can be explained by the fact that other properties of the hydrogels besides stiffness can influence cell adhesion and proliferation. Indeed, the hydrogels' chemical composition, texture, and permeability can all play a role in the ability of cells to attach and grow on the surface of the hydrogels[30]. As our hydrogels contained gelatin derived from collagen, a significant component of the extracellular matrix of tissues, the gelatin can provide a favorable substrate surface for cell adhesion and promote cell growth[31]. Moreover, it is possible that the difference in stiffness between the hydrogels is not significant enough to have an impact on cell adhesion and proliferation[32]. Finally, it is also possible that the DPSCs and MG-63 used in the experiment have different tolerances to hydrogel stiffness. Some cells may be more sensitive than others to changes in stiffness, which could explain why we did not observe a significant difference in cell adhesion and proliferation on low and high hydrogel stiffness, as reported previously [33].

3.3. Cell Morphology

The adhesion to and growth on the extracellular matrix may modulate the cell morphology. For this purpose, we analyzed the osteoblast ultrastructure after growth on the Alg-Gel hydrogels and subjected them to SEM analysis. As shown in Figure 5. the cells exhibited rounded and spherical morphology and were growing as grapes as bone-like nodules. These results suggest that the stiffness of hydrogels did not negatively influence the cell shape and support those showing that cells cultured on soft hydrogels exhibited a rounded and spherical shape[32]. Overall, our study showed the possibility of optimizing Alg-Gel hydrogel stiffness without affecting the cell morphology of DPSCs or MG-63.

 doi:10.20944/preprints202403.1674.v1

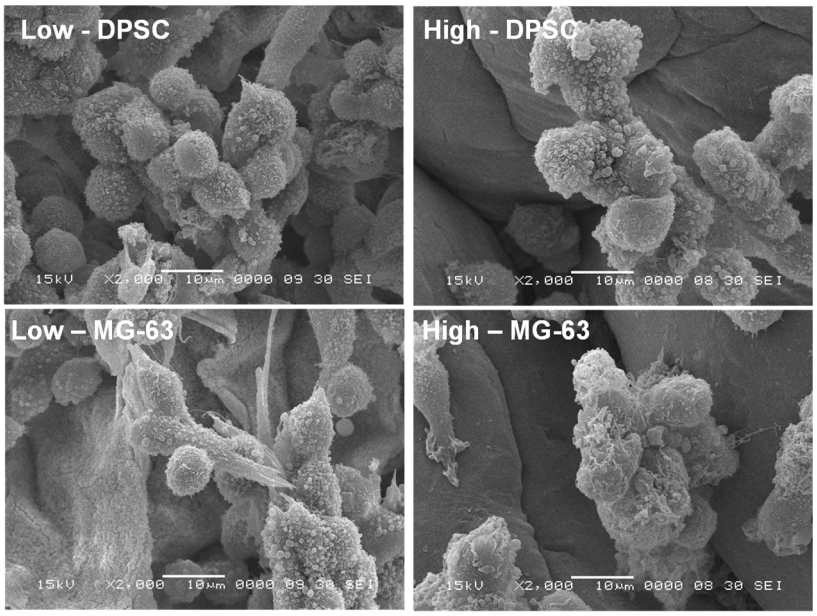

Figure 5. SEM images of DPSCs and MG-63 cells adhering to two hydrogels of different stiffness after 14 days of incubation, as observed by SEM. Arrows indicate cells adhering to the hydrogels.

However, it is possible that the stiffness of the hydrogels does not directly influence the morphology of these cells because the cells have an intrinsic ability to adapt their shape and structure to their environment[34],[35]. Indeed, cells can sense their environment through surface receptors, such as integrins, which allow them to detect the mechanical properties of their environment, including the stiffness of hydrogels[36]. The cells can then adapt their adhesion and motility in response to these mechanical properties[37],[38]. In addition, it is important to note that hydrogel stiffness may still indirectly affect the cells by altering the cell's response to biochemical signals and influencing cell differentiation[39].

3.4. Mineralization of Cells on Hydrogels

DPSCs and MG-63 mineralize in vitro and produce large extracellular calcium deposits. ALP activity and cell mineralization were used to assess osteoblast differentiation with Low and high hydrogels. Figures 6a and 6b showed the ALP activity of DPSC and MG-63 cells cultured on Low and High hydrogels. All results are normalized to 106 viable cells. ALP activity on both hydrogels increased with the duration of the culture period. Furthermore, ALP activity was higher on high hydrogels than on low hydrogels. A significantly high ALP activity was obtained with MG63 being cultured for 7 days on the high compared to the low hydrogels. However, ALP activity did not differ at 14 and 21 days of culture. This can be explained by the fact that ALP is an early osteogenic marker and that MG-63 cells are a positive control in our study[40],[41]. Interestingly, the use of DPSCs showed a significant increase of ALP activity at all tested culture periods, suggesting the high osteogenic capacity of the Alg-Gel hydrogels we designed, thus enabling bone formation.

Such bone formation can be evaluated using Calcium deposition through ARS staining[42],[43]. Figures 6c and 6d show that calcium deposition on Low and High hydrogels increased significantly from day 7 to day 21. Indeed, the CPC absorbance increased from 0.21 ± 0.01 on day 7 to 1.25 ± 0.05 on day 21 when the DPSC were cultured on the Low hydrogels. As for the High hydrogels, the CPC absorbance increased from 0.35 ± 0.02 at day 7 to 2.45 ± 0.04 at day 21. Similarly, for MG-63, CPC absorbance changed from 0.41 ± 0.01 and 0.65 ± 0.02 on day 7 to 1.92 ± 0.04 and 2.40 ± 0.02 on day 21 and on the Low and High hydrogels, respectively. The CPC activities are about twice as high in High than in the Low hydrogels for both cell types, confirming that the high-stiffness hydrogels promote Osteogenic differentiation[44],[35]. To confirm the osteogenic activity of the Alg-gel hydrogels, we performed an SEM analysis, which showed bone nodule formation (Figure 6f).

 doi:10.20944/preprints202403.1674.v1

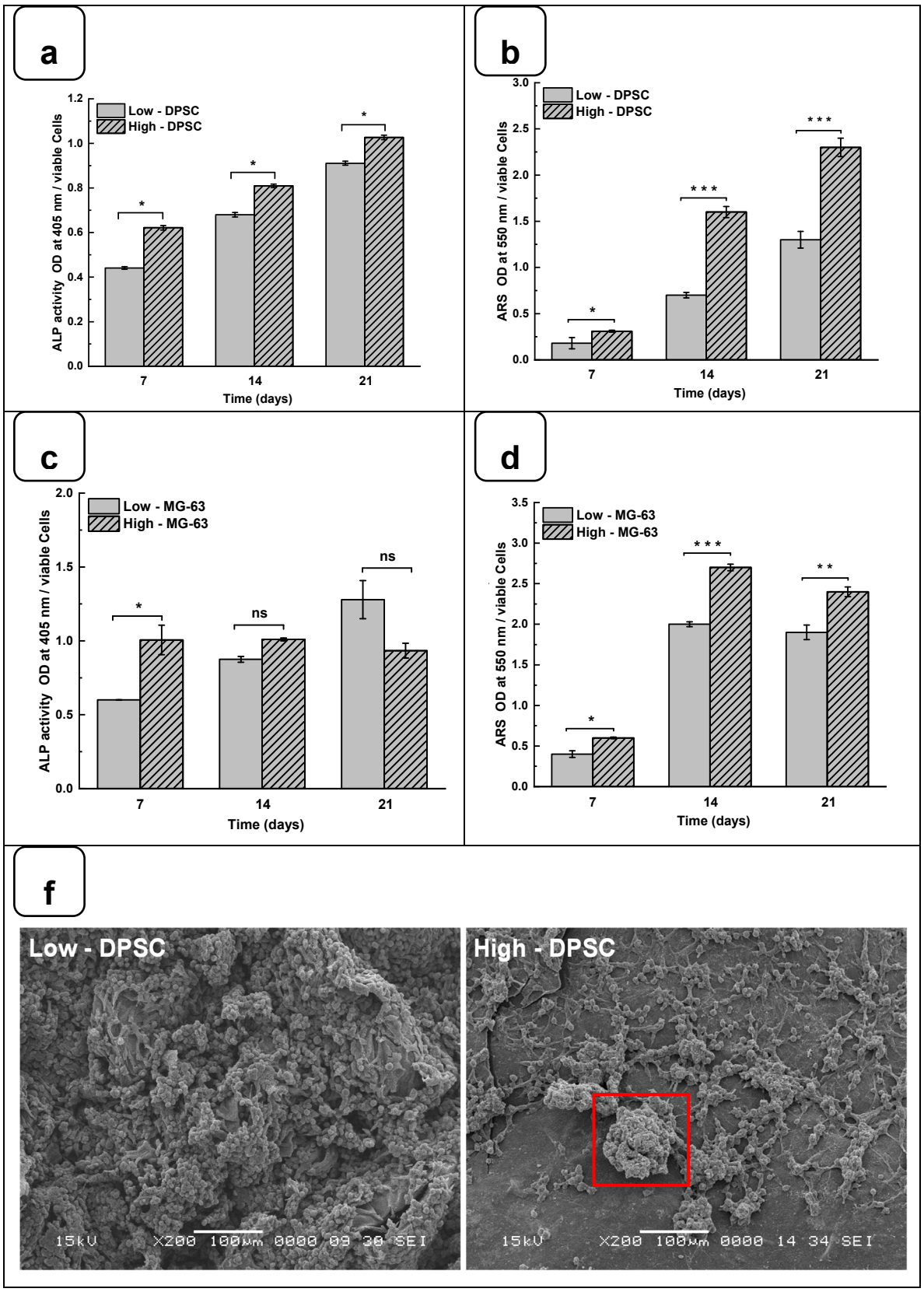

Figure 6. DPSC differentiation into osteoblast-like cells. (a) Alkaline phosphatase activity (b) ARS staining and CPC extraction. MG-63 differentiation into osteoblast-like cells. (c) Alkaline phosphatase activity (d) ARS staining and CPC extraction. (ODs were normalized by 10^6 viable cells). (f) SEM photomicrographs of osteoblast-type cells cultured for 7 days on low and high hydrogels. Nodular accretions with a diameter close to 100 µm were observed on the cells on the seventh day of culture with the high hydrogel. *p< 0.05, **p< 0.01, ***p< 0.001.

 doi:10.20944/preprints202403.1674.v1

Indeed, in the SEM photomicrographs, there were specific structures known as mineral nodules on hydrogels after a 7-day culture period of the osteoblasts. These nodules, appearing in specific areas indicated by squares on the images, exhibit an appearance reminiscent of cauliflower and have an average diameter of about 100 µm. Higher bone nodules were obtained compared to low-stiffness hydrogels (Figure 6f). Such mineralization rate was obtained at the different tested times, showing that high hydrogels exhibited a significantly higher mineralization rate than the low hydrogels. Such observation highlights the fact that the stiffness of the hydrogel plays a crucial role in the mineralization process, suggesting that the harder hydrogels provide a more conducive environment for bone nodule formation. Consequently, this finding underscores the importance of choosing the correct hydrogel stiffness, especially in biomedical applications where mineralization is crucial, such as bone regeneration.

4. Conclusions

This study highlights the significant impact of the mechanical properties of hydrogels, particularly their stiffness, on the fate of DPSCs. While variations in hydrogel stiffness did not significantly affect DPSC adhesion, proliferation, or morphology, they influenced their osteogenic potential. Hydrogels with greater stiffness demonstrated an ability to enhance the osteogenic activity of DPSCs, suggesting a promising avenue for guiding in vitro osteogenesis without the need for chemical-inducing agents. This advancement opens new perspectives for applying mechanobiology in regenerative medicine, particularly in developing more natural and less invasive bone regeneration strategies. The platforms based on the optimized Alg-Gel hydrogel could thus play a crucial role in future studies in cellular mechanobiology and clinical applications in tissue engineering and regenerative medicine.

Supplementary Materials: The following supporting information can be downloaded at the website of this paper posted on Preprints.org.

Author Contributions: Conceptualization, M.R, R.F, Z.F., and R.LM methodology, Z.F and M.R.; software, Z.F.; validation M.R, R.F, D.M., F.C, and Z.F; formal analysis, Z.F, R.LM., and S.A, investigation, Z.F; resources M.R and R.F.; data curation, Z.F, R.LM., and S.A; writing—original draft preparation, Z.F., and MR; writing—review and editing, R.F., F.C, D.M and Z.F.; visualization, M.R., R.F., F.C., and Z.F.; supervision, M.R., R.F., and F.C.; project administration, M.R. and F.C.; funding acquisition, M.R, R.F., and F.C. All authors have read and agreed to the published version of the manuscript.

Acknowledgments: This research was supported by a grant from Colgate-Palmolive (CARE), from Fonds Emile-Beaulieu, from the Natural Sciences and Engineering Research Council of Canada (NSERC)-Alliance grant (ALLRP 561197) to MR, and a Discovery Grant to DM. The authors are thankful to Jabrane Azelmat (GREB, FMD - Université Laval) for his contribution to the fluorescence microscopy experiments. The protocol figure was made using the free version of the software Biorender.

References

1. Arjmand, M.; Ardeshirylajimi, A.; Maghsoudi, H.; Azadian, E. Osteogenic Differentiation Potential of Mesenchymal Stem Cells Cultured on Nanofibrous Scaffold Improved in the Presence of Pulsed Electromagnetic Field. *J. Cell. Physiol.* **2018**, *233*, 1061–1070, doi:10.1002/jcp.25962.
2. Ye, J.; Yang, G.; Zhang, J.; Xiao, Z.; He, L.; Zhang, H.; Liu, Q. Preparation and Characterization of Gelatin-Polysaccharide Composite Hydrogels for Tissue Engineering. *PeerJ* **2021**, *9*, e11022, doi:10.7717/peerj.11022.
3. Lee, J.; Abdeen, A.A.; Zhang, D.; Kilian, K.A. Directing Stem Cell Fate on Hydrogel Substrates by Controlling Cell Geometry, Matrix Mechanics and Adhesion Ligand Composition. *Biomaterials* **2013**, *34*, 8140–8148, doi:10.1016/j.biomaterials.2013.07.074.
4. Nabavinia, M.; Khoshfetrat, A.B.; Naderi-Meshkin, H. Nano-Hydroxyapatite-Alginate-Gelatin Microcapsule as a Potential Osteogenic Building Block for Modular Bone Tissue Engineering. *Mater. Sci. Eng. C* **2019**, *97*, 67–77, doi:10.1016/j.msec.2018.12.033.
5. Zhao, W.; Li, X.; Liu, X.; Zhang, N.; Wen, X. Effects of Substrate Stiffness on Adipogenic and Osteogenic Differentiation of Human Mesenchymal Stem Cells. *Mater. Sci. Eng. C* **2014**, *40*, 316–323, doi:10.1016/j.msec.2014.03.048.

6. Žigon-Branc, S.; Markovic, M.; Van Hoorick, J.; Van Vlierberghe, S.; Dubruel, P.; Zerobin, E.; Baudis, S.; Ovsianikov, A. Impact of Hydrogel Stiffness on Differentiation of Human Adipose-Derived Stem Cell Microspheroids. *Tissue Eng. Part A* **2019**, *25*, 1369–1380, doi:10.1089/ten.tea.2018.0237.
7. Kamguyan, K.; Katbab, A.A.; Mahmoudi, M.; Thormann, E.; Zajforoushan Moghaddam, S.; Moradi, L.; Bonakdar, S. An Engineered Cell-Imprinted Substrate Directs Osteogenic Differentiation in Stem Cells. *Biomater. Sci.* **2018**, *6*, 189–199, doi:10.1039/C7BM00733G.
8. Witkowska-Zimny, M.; Walenko, K.; Wrobel, E.; Mrowka, P.; Mikulska, A.; Przybylski, J. Effect of Substrate Stiffness on the Osteogenic Differentiation of Bone Marrow Stem Cells and Bone-Derived Cells: Substrate Stiffness Affects Cell Osteogenesis. *Cell Biol. Int.* **2013**, *37*, 608–616, doi:10.1002/cbin.10078.
9. De Bartolo, L.; Mantovani, D. Bioartificial Organs: Ongoing Research and Future Trends. *Cells Tissues Organs* **2022**, 125–127, doi:10.1159/000518251.
10. Fernandez de Grado, G.; Keller, L.; Idoux-Gillet, Y.; Wagner, Q.; Musset, A.-M.; Benkirane-Jessel, N.; Bornert, F.; Offner, D. Bone Substitutes: A Review of Their Characteristics, Clinical Use, and Perspectives for Large Bone Defects Management. *J. Tissue Eng.* **2018**, *9*, 204173141877681, doi:10.1177/2041731418776819.
11. Gonzalez-Fernandez, T.; Sikorski, P.; Leach, J.K. Bio-Instructive Materials for Musculoskeletal Regeneration. *Acta Biomater.* **2019**, *96*, 20–34, doi:10.1016/j.actbio.2019.07.014.
12. Gonzalez-Fernandez, T.; Tenorio, A.J.; Campbell, K.T.; Silva, E.A.; Leach, J.K. Alginate-Based Bioinks for 3D Bioprinting and Fabrication of Anatomically Accurate Bone Grafts. *Tissue Eng. Part A* **2021**, *27*, 1168–1181, doi:10.1089/ten.tea.2020.0305.
13. Maisani, M.; Pezzoli, D.; Chassande, O.; Mantovani, D. Cellularizing Hydrogel-Based Scaffolds to Repair Bone Tissue: How to Create a Physiologically Relevant Micro-Environment? *J. Tissue Eng.* **2017**, *8*, 204173141771207, doi:10.1177/2041731417712073.
14. Vining, K.H.; Mooney, D.J. Mechanical Forces Direct Stem Cell Behaviour in Development and Regeneration. *Nat. Rev. Mol. Cell Biol.* **2017**, *18*, 728–742, doi:10.1038/nrm.2017.108.
15. Łabowska, M.B.; Cierluk, K.; Jankowska, A.M.; Kulbacka, J.; Detyna, J.; Michalak, I. A Review on the Adaption of Alginate-Gelatin Hydrogels for 3D Cultures and Bioprinting. *Materials* **2021**, *14*, 858, doi:10.3390/ma14040858.
16. Lee, K.Y.; Mooney, D.J. Alginate: Properties and Biomedical Applications. *Prog. Polym. Sci.* **2012**, *37*, 106–126, doi:10.1016/j.progpolymsci.2011.06.003.
17. Sahiner, N.; Sagbas, S.; Sahiner, M.; Silan, C. P(TA) Macro-, Micro-, Nanoparticle-Embedded Super Porous p(HEMA) Cryogels as Wound Dressing Material. *Mater. Sci. Eng. C* **2017**, *70*, 317–326, doi:10.1016/j.msec.2016.09.025.
18. Rongen, J.J.; van Bochove, B.; Hannink, G.; Grijpma, D.W.; Buma, P. Degradation Behavior of, and Tissue Response to Photo-Crosslinked Poly(Trimethylene Carbonate) Networks: TISSUE RESPONSE TO PHOTO-CROSSLINKED POLY(TRIMETHYLENE CARBONATE) NETWORKS. *J. Biomed. Mater. Res. A* **2016**, *104*, 2823–2832, doi:10.1002/jbm.a.35826.
19. Wei, B.; Wang, W.; Liu, X.; Xu, C.; Wang, Y.; Wang, Z.; Xu, J.; Guan, J.; Zhou, P.; Mao, Y. Gelatin Methacrylate Hydrogel Scaffold Carrying Resveratrol-Loaded Solid Lipid Nanoparticles for Enhancement of Osteogenic Differentiation of BMSCs and Effective Bone Regeneration. *Regen. Biomater.* **2021**, *8*, rbab044, doi:10.1093/rb/rbab044.
20. Yu, H.; Zhang, X.; Song, W.; Pan, T.; Wang, H.; Ning, T.; Wei, Q.; Xu, H.H.K.; Wu, B.; Ma, D. Effects of 3-Dimensional Bioprinting Alginate/Gelatin Hydrogel Scaffold Extract on Proliferation and Differentiation of Human Dental Pulp Stem Cells. *J. Endod.* **2019**, *45*, 706–715, doi:10.1016/j.joen.2019.03.004.
21. Akbari, S.; Taghavi, S.M. From Breakup to Coiling and Buckling Regimes in Buoyant Viscoplastic Injections. *J. Fluid Mech.* **2022**, *940*, A42, doi:10.1017/jfm.2022.254.
22. Filipović, V.V.; Babić Radić, M.M.; Vuković, J.S.; Vukomanović, M.; Rubert, M.; Hofmann, S.; Müller, R.; Tomić, S.Lj. Biodegradable Hydrogel Scaffolds Based on 2-Hydroxyethyl Methacrylate, Gelatin, Poly(β-Amino Esters), and Hydroxyapatite. *Polymers* **2021**, *14*, 18, doi:10.3390/polym14010018.
23. Li, F.; Li, J.; Song, X.; Sun, T.; Mi, L.; Liu, J.; Xia, X.; Bai, N.; Li, X. Alginate/Gelatin Hydrogel Scaffold Containing nCeO2 as a Potential Osteogenic Nanomaterial for Bone Tissue Engineering. *Int. J. Nanomedicine* **2022**, *Volume 17*, 6561–6578, doi:10.2147/IJN.S388942.
24. Sosnik, A. Alginate Particles as Platform for Drug Delivery by the Oral Route: State-of-the-Art. *ISRN Pharm.* **2014**, *2014*, 1–17, doi:10.1155/2014/926157.
25. Chen, Z.; Lv, Y. Gelatin/Sodium Alginate Composite Hydrogel with Dynamic Matrix Stiffening Ability for Bone Regeneration. *Compos. Part B Eng.* **2022**, *243*, 110162, doi:10.1016/j.compositesb.2022.110162.
26. Naghieh, S.; Karamooz-Ravari, M.R.; Sarker, M.; Karki, E.; Chen, X. Influence of Crosslinking on the Mechanical Behavior of 3D Printed Alginate Scaffolds: Experimental and Numerical Approaches. *J. Mech. Behav. Biomed. Mater.* **2018**, *80*, 111–118, doi:10.1016/j.jmbbm.2018.01.034.
27. Stojkov, G.; Niyazov, Z.; Picchioni, F.; Bose, R.K. Relationship between Structure and Rheology of Hydrogels for Various Applications. *Gels* **2021**, *7*, 255, doi:10.3390/gels7040255.

28. Gregory, T.; Benhal, P.; Scutte, A.; Quashie, D.; Harrison, K.; Cargill, C.; Grandison, S.; Savitsky, M.J.; Ramakrishnan, S.; Ali, J. Rheological Characterization of Cell-Laden Alginate-Gelatin Hydrogels for 3D Biofabrication. *J. Mech. Behav. Biomed. Mater.* **2022**, *136*, 105474, doi:10.1016/j.jmbbm.2022.105474.
29. Serafin, A.; Culebras, M.; Collins, M.N. Synthesis and Evaluation of Alginate, Gelatin, and Hyaluronic Acid Hybrid Hydrogels for Tissue Engineering Applications. *Int. J. Biol. Macromol.* **2023**, *233*, 123438, doi:10.1016/j.ijbiomac.2023.123438.
30. Chen, X.; Aledia, A.S.; Popson, S.A.; Him, L.; Hughes, C.C.W.; George, S.C. Rapid Anastomosis of Endothelial Progenitor Cell–Derived Vessels with Host Vasculature Is Promoted by a High Density of Cotransplanted Fibroblasts. *Tissue Eng. Part A* **2010**, *16*, 585–594, doi:10.1089/ten.tea.2009.0491.
31. Chai, Q.; Jiao, Y.; Yu, X. Hydrogels for Biomedical Applications: Their Characteristics and the Mechanisms behind Them. *Gels* **2017**, *3*, 6, doi:10.3390/gels3010006.
32. Luo, T.; Tan, B.; Zhu, L.; Wang, Y.; Liao, J. A Review on the Design of Hydrogels With Different Stiffness and Their Effects on Tissue Repair. *Front. Bioeng. Biotechnol.* **2022**, *10*, 817391, doi:10.3389/fbioe.2022.817391.
33. Loessner, D.; Stok, K.S.; Lutolf, M.P.; Hutmacher, D.W.; Clements, J.A.; Rizzi, S.C. Bioengineered 3D Platform to Explore Cell–ECM Interactions and Drug Resistance of Epithelial Ovarian Cancer Cells. *Biomaterials* **2010**, *31*, 8494–8506, doi:10.1016/j.biomaterials.2010.07.064.
34. Discher, D.E.; Janmey, P.; Wang, Y. Tissue Cells Feel and Respond to the Stiffness of Their Substrate. *Science* **2005**, *310*, 1139–1143, doi:10.1126/science.1116995.
35. Sun, M.; Chi, G.; Li, P.; Lv, S.; Xu, J.; Xu, Z.; Xia, Y.; Tan, Y.; Xu, J.; Li, L.; et al. Effects of Matrix Stiffness on the Morphology, Adhesion, Proliferation and Osteogenic Differentiation of Mesenchymal Stem Cells. *Int. J. Med. Sci.* **2018**, *15*, 257–268, doi:10.7150/ijms.21620.
36. Pelham, R.J.; Wang, Y. Cell Locomotion and Focal Adhesions Are Regulated by Substrate Flexibility. *Proc. Natl. Acad. Sci.* **1997**, *94*, 13661–13665, doi:10.1073/pnas.94.25.13661.
37. Schwarz, U.S.; Safran, S.A. Physics of Adherent Cells. *Rev. Mod. Phys.* **2013**, *85*, 1327–1381, doi:10.1103/RevModPhys.85.1327.
38. Trappmann, B.; Gautrot, J.E.; Connelly, J.T.; Strange, D.G.T.; Li, Y.; Oyen, M.L.; Cohen Stuart, M.A.; Boehm, H.; Li, B.; Vogel, V.; et al. Extracellular-Matrix Tethering Regulates Stem-Cell Fate. *Nat. Mater.* **2012**, *11*, 642–649, doi:10.1038/nmat3339.
39. Chaudhuri, O.; Koshy, S.T.; Branco da Cunha, C.; Shin, J.-W.; Verbeke, C.S.; Allison, K.H.; Mooney, D.J. Extracellular Matrix Stiffness and Composition Jointly Regulate the Induction of Malignant Phenotypes in Mammary Epithelium. *Nat. Mater.* **2014**, *13*, 970–978, doi:10.1038/nmat4009.
40. Beck, G.R.; Zerler, B.; Moran, E. Phosphate Is a Specific Signal for Induction of Osteopontin Gene Expression. *Proc. Natl. Acad. Sci.* **2000**, *97*, 8352–8357, doi:10.1073/pnas.140021997.
41. Ginebra, M.P.; Traykova, T.; Planell, J.A. Calcium Phosphate Cements as Bone Drug Delivery Systems: A Review. *J. Controlled Release* **2006**, *113*, 102–110, doi:10.1016/j.jconrel.2006.04.007.
42. Akkouch, A.; Zhang, Z.; Rouabhia, M. Engineering Bone Tissue Using Human Dental Pulp Stem Cells and an Osteogenic Collagen-Hydroxyapatite-Poly (L -Lactide-Co-ε-Caprolactone) Scaffold. *J. Biomater. Appl.* **2014**, *28*, 922–936, doi:10.1177/0885328213486705.
43. Alipour, M.; Firouzi, N.; Aghazadeh, Z.; Samiei, M.; Montazersaheb, S.; Khoshfetrat, A.B.; Aghazadeh, M. The Osteogenic Differentiation of Human Dental Pulp Stem Cells in Alginate-Gelatin/Nano-Hydroxyapatite Microcapsules. *BMC Biotechnol.* **2021**, *21*, 6, doi:10.1186/s12896-020-00666-3.
44. Jones, J.R.; Tsigkou, O.; Coates, E.E.; Stevens, M.M.; Polak, J.M.; Hench, L.L. Extracellular Matrix Formation and Mineralization on a Phosphate-Free Porous Bioactive Glass Scaffold Using Primary Human Osteoblast (HOB) Cells. *Biomaterials* **2007**, *28*, 1653–1663, doi:10.1016/j.biomaterials.2006.11.022.